Atmos. Chem. Phys., 8, 6577–6586, 2008
www.atmos-chem-phys.net/8/6577/2008/

Atmospheric Chemistry and Physics

Validation of OMI tropospheric NO_2 column data using MAX-DOAS measurements deep inside the North China Plain in June 2006: Mount Tai Experiment 2006

H. Irie[1], Y. Kanaya[1], H. Akimoto[1], H. Tanimoto[2], Z. Wang[3], J. F. Gleason[4], and E. J. Bucsela[5]

[1]Frontier Research Center for Global Change, Japan Agency for Marine-Earth Science and Technology, 3173-25 Showa-machi, Kanazawa-ku, Yokohama, Kanagawa 236-0001, Japan
[2]National Institute for Environmental Studies, 16-2, Onogawa, Tsukuba, Ibaraki 305-8506, Japan
[3]LAPC/NZC, Institute of Atmospheric Physics, Chinese Academy of Sciences, Beijing, 100029, China
[4]Atmospheric Chemistry and Dynamics branch, NASA Goddard Space Flight Center, Greenbelt, MD 20771-0000, USA
[5]SRI International, Menlo Park, CA 94107, USA

Received: 4 March 2008 – Published in Atmos. Chem. Phys. Discuss.: 25 April 2008
Revised: 23 July 2008 – Accepted: 6 October 2008 – Published: 17 November 2008

Abstract. A challenge for the quantitative analysis of tropospheric nitrogen dioxide (NO_2) column data from satellite observations is posed partly by the lack of satellite-independent observations for validation. We performed such observations of the tropospheric NO_2 column using the ground-based Multi-Axis Differential Optical Absorption Spectroscopy (MAX-DOAS) technique in the North China Plain (NCP) from 29 May to 29 June, 2006. Comparisons between tropospheric NO_2 columns measured by MAX-DOAS and the Ozone Monitoring Instrument (OMI) onboard the Aura satellite indicate that OMI data (the standard product, version 3) over NCP may have a positive bias of 1.6×10^{15} molecules cm^{-2} (20%), yet within the uncertainty of the OMI data. Combining these results with literature validation results for the US, Europe, and Pacific Ocean suggests that a bias of +20%/−30% is a reasonable estimate, accounting for different regions.

1 Introduction

Since 1995, satellite observations have provided tropospheric column data for nitrogen dioxide (NO_2) on a global scale (e.g., Richter et al., 2005). The satellite observations have been shown to be crucial, for instance, to the estimation of recent trends in tropospheric NO_2 over several important regions, including the North China Plain (NCP) of the People's Republic of China (Richter et al., 2005; Irie et al., 2005; van der A et al., 2006), and to the systematic evaluation of global atmospheric chemistry models (van Noije et al., 2006). However, although a quantitative basis for analyzing satellite data should be provided by comparisons with other independent measurements, such satellite-independent measurements are very limited. Some satellite-independent measurements were made over the U.S., Europe, and Pacific Ocean (Brinksma et al., 2008; Bucsela et al., 2008; Celarier et al., 2008), but none over NCP (Irie et al., 2005). In addition, tropospheric column data can be obtained only at specific local times (LTs) under cloud-free conditions, because of the satellite orbit and interference by clouds. Furthermore, it is generally very difficult to derive vertical profile information in the troposphere from satellite observations.

To cover these shortcomings in satellite observations of tropospheric NO_2, we performed ground-based Multi-Axis Differential Optical Absorption Spectroscopy (MAX-DOAS) measurements at two sites at the base and summit of Mt. Tai in NCP between 29 May and 29 June, 2006. The base site is referred to as "Tai'an" (36.2° N, 117.1° E, 126 m a.s.l.) and the mountaintop site located only 10 km north of Tai'an is referred to as "Mt. Tai" (36.3° N, 117.1° E, 1534 m a.s.l.). The measurements were made as a part of an intensive field measurement campaign (Mount Tai Experiment 2006). The retrieval of the tropospheric NO_2 column is performed using the vertical profiles of the box-air-mass-factor (A_{box}), which is defined as the air mass factor for a given layer (Wagner et al., 2007). The A_{box} profile is determined from MAX-DOAS itself, as the analysis of absorption by the oxygen collision complex (O_2-O_2, or O_4) gives a vertical profile of the aerosol extinction coefficient (AEC) that controls the effective path of sunlight reaching the MAX-DOAS system (Irie et al.,

Correspondence to: H. Irie
(irie@jamstec.go.jp)

2008). In the present study, we first assess the MAX-DOAS measurements by two approaches: (1) using the aerosol optical depth (AOD) data (Collection 005) from the Moderate Resolution Imaging Spectrometer (MODIS) to verify the determined A_{box} profiles and (2) using the NO_2 volume mixing ratio (VMR) data obtained in situ by a chemiluminescence technique at the top of Mt. Tai to confirm the NO_2 retrieval. On the basis of these assessments, the standard product (SP) of tropospheric NO_2 column data (version 3) obtained by the Ozone Monitoring Instrument (OMI) (Levelt et al., 2006) onboard NASA's Earth Observing System (EOS) Aura satellite over NCP is validated for the first time, through comparisons with MAX-DOAS data. The OMI data are characterized also from the viewpoint of the diurnal variation pattern of the tropospheric NO_2 column based on its measurements by MAX-DOAS.

2 Measurements

2.1 MAX-DOAS

From 29 May to 29 June 2006, we performed MAX-DOAS measurements at two sites, Tai'an and Mt. Tai, in NCP. At Tai'an, we operated a MAX-DOAS instrument employing a miniaturized ultraviolet/visible (UV/VIS) spectrometer (B&W TEK Inc., BTC111), a single telescope, and a movable mirror, to conduct sequential measurements of scattered sunlight at five different elevation angles (ELs) of 5°, 10°, 20°, 30°, and 90° every 30 min. The line of sight (LOS) for off-axis geometries was directed northward. On the other hand, the MAX-DOAS system operated at Mt. Tai employed a two-dimensional CCD (charge-coupled device) array detector (Andor Technology, DV-420A-OE; 1024×256 pixels) and five telescopes, which were all directed south but with different ELs fixed at −5°, 5°, 10°, 20°, and 30°. To acquire a reference spectrum with the same instrument line shape as that of the off-axis measurements, a mirror was periodically inserted into the field of view (FOV) of each telescope, directing the viewing path to the zenith sky (EL=90°). For each telescope, a 6-min zenith-sky measurement was made every 30 min. The five different measured spectra were projected onto the two-dimensional CCD detector simultaneously, with 1024 pixels for wavelengths of 425–490 nm (x-direction) and 30 pixels for each of the five telescopes (y-direction). Both MAX-DOAS systems placed at Tai'an and Mt. Tai were operated throughout the day. Wavelength calibration using a high-resolution solar spectrum (Kurucz et al., 1984) indicated that the spectral resolution (full width at half maximum (FWHM)) was about 0.4–0.5 and 0.2–0.3 nm at Tai'an and Mt. Tai, respectively. More information on these MAX-DOAS instruments can be found elsewhere (Irie et al., 2008; Inomata et al., 2008).

We used a common retrieval algorithm for measurements at both Tai'an and Mt. Tai, as described below. To the fitting window of 460–490 nm we applied the DOAS spectral fitting algorithm described by Irie et al. (2008). The quantity retrieved with this DOAS method is the so-called differential slant column density (ΔSCD), which is defined as the difference between the column concentration integrated along the sunlight path measured at a low EL (EL<90°) and that at EL=90°. The window 460–490 nm was chosen to retrieve NO_2 and O_4 ΔSCD values from the same fitting window, minimizing the difference between wavelengths for NO_2 and O_4 air mass factors. The retrieval algorithm took into account absorption by trace gases NO_2, O_4, O_3, and H_2O, and the Ring and undersampling effects. For Tai'an, NO_2 and O_4 ΔSCD errors estimated from fitting residuals were usually about 1.5×10^{14} molecules cm^{-2} and 1.0×10^{41} molecules^2 cm^{-5}, respectively. Those for Taishan were 0.7×10^{14} molecules cm^{-2} and 0.4×10^{41} molecules^2 cm^{-5}, respectively.

The O_4 ΔSCD values were next converted using our aerosol retrieval algorithm (Irie et al., 2008) to the AOD and the vertical profile of the AEC at a wavelength of 476 nm, which corresponds to the O_4 cross-section-weighted mean wavelength over 460–490 nm. The aerosol retrieval was made using the optimal estimation method (Rodgers, 2000; Irie et al., 2008). A lookup table (LUT) for the vertical profile of A_{box}, which characterizes the ratio of partial slant to vertical columns for a given layer, was created by a three-dimensional Monte Carlo radiative transfer model, MCARaTS (Iwabuchi, 2006), and used to find the optimal aerosol and A_{box} profiles that account for O_4 ΔSCD values measured at all ELs. MCARaTS is a parallelized three-dimensional radiative transfer model utilizing the forward-propagating Monte Carlo photon transport algorithm. Radiances were calculated by integrating the contributions from each event of scattering or source emission, according to the local estimation method (Marchuk et al., 1980). For a given layer, A_{box} was calculated as an intensity-weighted average path length. High-precision calculations of the A_{box} profiles were made by simulating 10^6 photons. The collision-forcing method of Iwabuchi (2006) was used to reduce the computational noise in the cases of an optically thin atmosphere. The A_{box} calculations by MCARaTS have been validated through comparisons with other radiative transfer models (Wagner et al., 2007). To simulate a realistic atmosphere, we considered the surface altitude at the measurement site and the altitude where the instrument was located. The present LUT contains more than 300 000 A_{box} profiles as functions of the aerosol profile scenario and observation geometry. Each profile has 72 layers for altitudes up to 100 km, with a layer thickness of 100 m at altitudes below 5.1 km. The radiative transfer model calculations made in the present study assume a single scattering albedo of 0.90, an asymmetry parameter of 0.65, and a surface albedo of 0.10. The overall intrinsic uncertainty in the retrieved AOD, including the impact of these assumptions, was estimated generally to be 30% (Irie et al., 2008). It should be noted, however, that the MAX-DOAS AOD can

Table 1. Median values of the absolute and relative errors (± (systematic error) ± (1σ random error)), the maximum box-air-mass-factors ($A_{\mathrm{box,max}}$), and the horizontal distances (D) for MAX-DOAS NO_2 measurements at Tai'an.

	Abs. err.[a]	Rel. err. (%)	$A_{\mathrm{box,max}}$	D(km)
VCD	±1.0±0.5	±11±5	–	–
VMR 0–1 km	±0.3±0.3	±9±11	3.8	3.7
VMR 1–2 km	±0.1±0.2	±8±28	2.7	2.5

[a] Units are 10^{15} molecules cm^{-2} and ppbv for VCD and VMR, respectively.

Table 2. Same as Table 1, but for MAX-DOAS measurements at Mt. Tai.

	Abs. err.[a]	Rel. err. (%)	$A_{\mathbf{box},\mathrm{max}}$	D(km)
VCD	(±0.6±1.1)[b]	(±7±12)[b]	–	–
VMR 0–1 km	(±0.3±0.6)[b]	(±8±19)[b]	1.2	0.7
VMR 1–2 km	±0.1±0.3	±10±47	5.1	5.0

[a] Units are 10^{15} molecules cm^{-2} and ppbv for VCD and VMR, respectively.
[b] Note that the errors can be greater due to the insufficient penetration of the measured sunlight for the 0–1-km layer, as discussed in the text.

be underestimated when optically thick aerosols are present at high altitudes (Irie et al., 2008). While MAX-DOAS measurements are very insensitive to high-altitude clouds (above ∼2 km), it is likely that the retrieved AOD includes a 30%-reduced contribution of cloud optical depth at lower altitudes (Irie et al., 2008). These effects, however, do not essentially impact the OMI validation results, as discussed later.

Since the A_{box} profile is a function of the aerosol profile in the LUT, the A_{box} is also uniquely determined by the aerosol retrieval method. Using the A_{box} profiles and a nonlinear iterative inversion method very similar to that of the aerosol retrieval, we converted the NO_2 ΔSCD values to the tropospheric vertical column density (VCD) and the vertical profile of NO_2. We defined the measurement vector ($\boldsymbol{y}$; representing quantities to be fitted) and the state vector ($\boldsymbol{x}$; representing quantities to be retrieved) as

$$\boldsymbol{y} = (\mathrm{NO_2\Delta SCD}(\Omega_1)...\mathrm{NO_2\Delta SCD}(\Omega_n))^T \quad \text{and} \tag{1}$$

$$\boldsymbol{x} = (\mathrm{VCD}\, f_1 f_2 f_3)^T, \tag{2}$$

respectively, where n is the number of measurements in a 30-min interval, which corresponds to a complete sequence of ELs, and Ω is the observation geometry vector consisting of three components: the solar zenith angle (SZA), the relative azimuth angle (RAA), and EL. RAA is the azimuth angle between the telescope direction and the Sun. The f values are the parameters determining the shape of the vertical profile and are defined to range between 0 and 1. Thereby, partial VCDs for 0–1, 1–2, and 2–3 km can be described as $\mathrm{VCD}\, f_1$, $\mathrm{VCD}(1-f_1)f_2$, and $\mathrm{VCD}(1-f_1)(1-f_2)f_3$, respectively, and the partial VCD at 3–15 km as $\mathrm{VCD}(1-f_1)(1-f_2)(1-f_3)$, where VCD is defined as the tropospheric column at altitudes of 0–15 km.

From the given partial VCD at 3–15 km, we determined the NO_2 profile for a layer from 3 to 15 km assuming the value at 15 km and an exponential profile shape. Similarly, we determined profiles for layers of 2–3, 1–2, and 0–1 km, completing the continuous NO_2 vertical profile from the surface to 15 km. An assumption of the stratospheric NO_2 (at 15–50 km), which might contribute to NO_2 ΔSCD values, was made based on a dataset from Halogen Occultation Experiment (HALOE) measurements at midlatitudes.

Note that the resulting partial VCD values, such as $\mathrm{VCD}\, f_1$ for the 0–1-km layer, gives the mean number concentration ($\mathrm{VCD}\, f_1\ \Delta z$, where Δz=1 km) for a given 1-km layer. This was converted to VMR using US Standard Atmosphere temperature and pressure data, which were scaled to match the surface values recorded at the location and time of the measurements.

An accurate error estimate is a major challenge for remote sensing measurements, including MAX-DOAS. For each retrieval, we estimated the random error from the retrieval covariance matrix. In this estimate, we used the measurement error covariance matrix constructed from the residual that arose in fitting the NO_2 ΔSCD values. This is because the residual was much larger than the NO_2 ΔSCD error quantified from the DOAS fitting residuals. The systematic error was estimated as the root-mean-squares of the changes that were found when we varied the AOD by an additional ±30%, biased ELs by ±0.2°, and doubled the assumed stratospheric amount of NO_2. We found that the systematic error was dominated by the AOD variation. At Tai'an, for example, the median error in VCD due to the change in AOD was 1.0×10^{15} molecules cm^{-2} (11%), whereas those for changes in EL and the stratospheric amount were both less than 0.1×10^{15} molecules cm^{-2} (<1%). Note that the error due to the AOD variation should include the impact of assumptions on single scattering albedo, asymmetry parameter, and surface albedo, as mentioned earlier. For all the measurements at Tai'an and Mt. Tai, the mean values of the random and systematic errors estimated in this way are summarized in Tables 1 and 2, respectively. In Tables 1 and 2, the mean values of the maximum A_{box} at different ELs for each retrieval ($A_{\mathrm{box,max}}$) and the mean horizontal distances (D), over which the measured sunlight traversed, are also shown for each layer. The D values were calculated as $\sqrt{A_{\mathrm{box,max}}^2 - 1}$, and both the $A_{\mathrm{box,max}}$ and D values provide a measure of the MAX-DOAS measurement sensitivity. Consistent with previous work showing that the highest

sensitivity of MAX-DOAS measurements occurs in the layer nearest the instrument (Hönninger et al., 2004; Frieß et al., 2006; Irie et al., 2008), the $A_{box,max}$ and D values at 0–1 km are larger than at 1–2 km for MAX-DOAS measurements at Tai'an. For the measurement geometry at Mt. Tai, the $A_{box,max}$ and D values for the 0–1-km layer are as small as 1.2 and 0.7 km, respectively, indicating that the measured sunlight could not penetrate deep inside the layer. Therefore, the following analyses use only the VMR data at 1–2 km, for measurements at Mt. Tai.

2.2 In situ NO/NO_x instrument

At the top of Mt. Tai, the NO_2 VMR was measured by a custom-built NO/NO_x instrument based on a chemiluminescence NO analyzer coupled with a NO_2-to-NO photolytic converter. NO was measured using a high-sensitivity chemiluminescence analyzer (Thermo Environmental Instruments Inc., 42 CTL). NO_2 was detected as NO following narrow-band photo-dissociation by a light-emitting diode (LED) between 390 and 405 nm (Droplet Measurement Technologies, BLC). The use of a LED-based converter is suitable for a field operation, especially at a mountainous site, because it has a longer lifetime, emits less heat, and consumes less energy than a conventional lamp does. The conversion efficiency of NO_2 was typically 50% at a flow rate of ~1 s.l.p.m. The time resolution was 3 min for each mode for NO and NO_2. Sensitivity and background levels of NO and NO_x were investigated in detail by the gas-phase titration (GPT) technique. National Institute for Environmental Studies (NIES) gas standards used were gravimetrically prepared at 2 ppmv and intercompared to National Oceanic and Atmospheric Administration (NOAA) standards. Agreement between NIES and NOAA standards was within 0.5%. For a 1-min integration the detection limit for NO was estimated to be ~100 pptv, and for NO_2 it was ~200 pptv. The instrument was computer-controlled for switching flow valves, lamp, sample and O_2 flows, and data acquisition.

2.3 OMI

The OMI instrument is a nadir-viewing imaging spectrometer measuring direct and atmosphere-backscattered sunlight in the UV/VIS range from 270 to 500 nm (Levelt et al., 2006). It was launched onboard the Aura satellite on 15 July 2004, and put into a Sun-synchronous, polar orbit at an altitude of about 705 km with an equator crossing time between 13:40 and 13:50 LT. OMI employs two two-dimensional CCD detectors that record the (ir)radiance spectrum in UV (270–310 nm and 310–365 nm) and VIS (365–500 nm) regions, respectively. Over the OMI FOV (114°), 60 discrete viewing angles are distributed perpendicular to the flight direction. The FOV corresponds to a 2600-km-wide spatial swath on the Earth's surface, achieving daily global measurements. Nadir spatial resolution ranges from 13×24 to 24×48 km^2, depending on the operation mode.

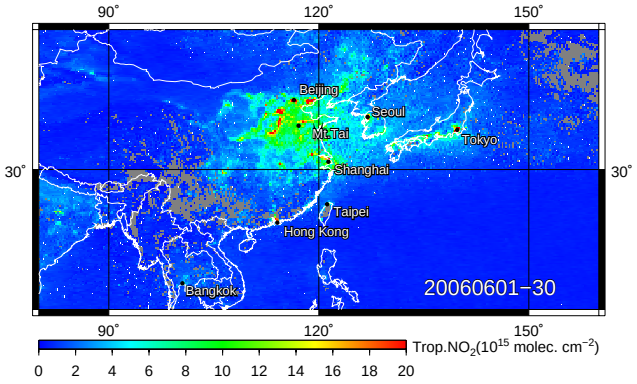

Fig. 1. Monthly mean tropospheric NO_2 columns measured by OMI in June 2006. Data with a cloud fraction less than 0.1 were plotted on a 0.25° (in latitude) × 0.25° (in longitude) grid. Values exceeding 20×10^{15} molecules cm^{-2} are shown in red. MAX-DOAS measurements were made at and near the location indicated by "Mt. Tai." Tai'an was located only 10 km south of Mt. Tai.

The present study uses the SP dataset (version 3) of OMI tropospheric NO_2 columns retrieved based on the methods described by Bucsela et al. (2006) and Celarier et al. (2008). We used the data referred to as "ColumnAmountNO_2Trop" in data files obtained from the NASA Goddard Earth Sciences Data and Information Services Center (GES-DISC). Another OMI SP data product, "ColumnAmountNO_2TropPolluted", was almost equivalent to the "ColumnAmountNO_2Trop" data for the dataset analyzed here, as the differences between the two values were very small ($<0.2\times10^{15}$ molecules cm^{-2}). A "below cloud" NO_2 column has been added for more realistic tropospheric column estimates, but only data with a cloud fraction less than 0.1 are analyzed below. For data obtained within 0.1° latitude and longitude of Tai'an in June 2006, the average of errors reported in the data files was 2.2×10^{15} molecules cm^{-2} (24%). Daily maps of OMI tropospheric NO_2 column data in June 2006 did not show significant stripes along satellite tracks passing over NCP. The monthly average map of the OMI tropospheric NO_2 columns for June 2006 is shown in Fig. 1. Pronounced high tropospheric NO_2 columns exceeding 10×10^{15} molecules cm^{-2} were extensively distributed over the NCP region, including MAX-DOAS measurement sites at/near Mt. Tai. In particular, considerable amounts of tropospheric NO_2 exceeding 20×10^{15} molecules cm^{-2} were observed around Beijing, Tanshan (east of Beijing), a mountain/NCP-edge area including Shijiazhuang, Xingtai, and Handan (southwest of Beijing), Jinan (north of Mt. Tai), and Shanghai.

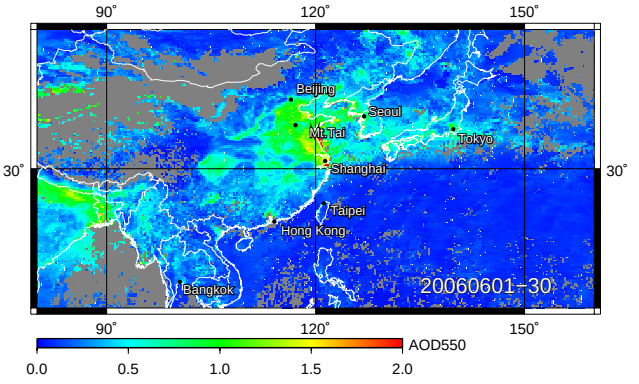

Fig. 2. Same as Fig. 1, but for AOD at 550 nm measured by MODIS instruments. The MODIS data with a cloud fraction less than 0.1 were used. Two datasets, from MODIS/Terra and MODIS/Aqua, have been unified.

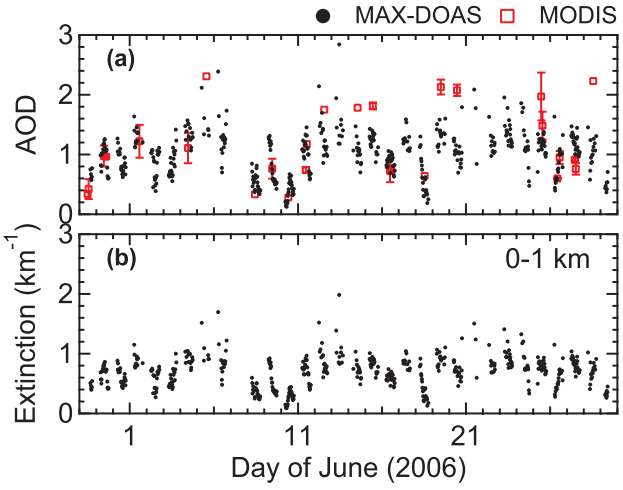

Fig. 3. **(a)** Time series of AOD values at 476 nm derived from MAX-DOAS measurements at Tai'an (black). Mean AOD values obtained by MODIS within 0.1° latitude and longitude of Tai'an are also shown in red. Error bars represent 1σ standard deviations. Two MODIS datasets from Terra and Aqua satellites have been averaged separately but are plotted with the same symbols for simplicity. The MODIS data with a cloud fraction less than 0.1 were used. The original MODIS AOD values at 470 nm have been converted to the values at 476 nm using the Ångström exponent. **(b)** Time series of MAX-DOAS-derived AEC values for the lowest 1-km layer above the surface is shown.

3 Results and discussion

3.1 Assessment of MAX-DOAS data

In this section, we describe the assessment of both the aerosol and NO_2 measurements made with the MAX-DOAS instrument. First, we use MODIS AOD data (Collection 005) to assess the MAX-DOAS aerosol retrievals that determine the A_{box} vertical profiles. According to a MODIS website at http://modis-atmos.gsfc.nasa.gov, it is most likely that the quality of the MODIS collection 005 AOD data has been improved since the Collection 004 dataset, which was validated using AERONET (Aerosol Robotic Network) measurements (Remer et al., 2005). Monthly mean AOD values at 550 nm measured by MODIS instruments for June 2006 are shown in Fig. 2. Both datasets from MODIS/Terra and MODIS/Aqua have been simply averaged. Similar to the tropospheric NO_2 map shown in Fig. 1, high AOD values occurred over large areas of the NCP. Peak AOD values are found in the southeastern part of NCP, presumably due to crop residue burning associated with the local harvest of winter wheat in this season, as discussed by Fu et al. (2007) using satellite formaldehyde (from GOME) and hot spot data (from ATSR) and the GEOS-Chem global chemical transport model.

In Fig. 3a, a time series of AOD values at 476 nm derived from the MAX-DOAS at Tai'an is compared with that of mean MODIS AOD data obtained within 0.1° latitude and longitude of Tai'an. Note that the plotted MODIS AOD values have been converted from the original AOD values at 470 nm using MODIS Ångström exponent data. The MODIS data with a cloud fraction less than 0.1 were used. Good agreement between MAX-DOAS and MODIS AOD values is seen, especially with respect to the pattern of temporal variation. This agreement is surprising under such considerably high-AOD conditions, where MAX-DOAS measurements show that the mean AEC value for the lowest 1-km layer was as high as 0.7 km^{-1} on average over the measurement period (Fig. 3b). The mean AEC value corresponds to a visibility of only 5.6 km, based on the Koschmieder equation (Jacobson, 1999).

Although the MAX-DOAS and MODIS measurements were both made under such severe conditions, positive correlations were obtained at MODIS AOD$<$1.2 (Fig. 4). The plotted MAX-DOAS values were obtained by interpolating two values measured within 30 min before and after MODIS measurements were made. For most cases with MODIS AOD$<$1.6, agreement is within 30%. However, significant deviations occur at MODIS AOD$>$1.2 for both comparisons with MODIS/Terra and MODIS/Aqua. Such large deviations are not expected to be due to an error in the MODIS data, because comprehensive comparisons have shown better agreement with AERONET measurements (Remer et al., 2005), suggesting an underestimate in MAX-DOAS AOD values. A similar tendency for occasional underestimation has been discussed in our previous work, where we have attributed it to the presence of optically thick aerosols at high altitudes and/or clouds in the lower troposphere (Irie et al., 2008).

As mentioned above, MODIS AOD data with a cloud fraction less than 0.1 have been compared to the MAX-DOAS AOD data in Figs. 3 and 4. In addition, for the analyzed 0.1°$\times$ 0.1° grid centered on Tai'an, standard deviations that may reflect spatial inhomogeneity of the optical depth due

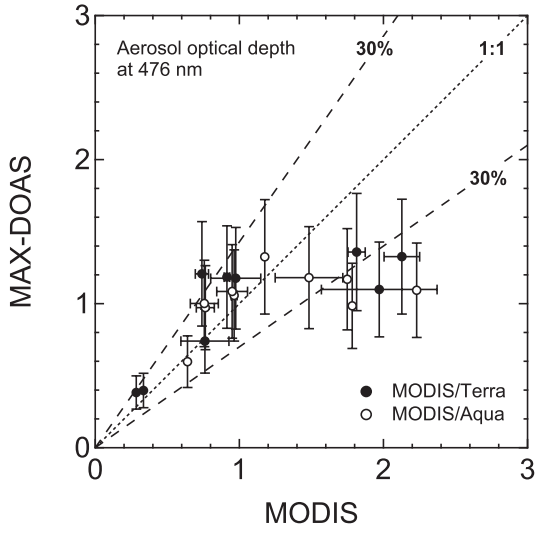

Fig. 4. Correlations between AOD values at 476 nm derived from MAX-DOAS and MODIS. Two MODIS datasets from Terra and Aqua are shown with solid and open symbols, respectively. The 1:1 relationship and the 30% range are represented by the dotted line and dashed lines, respectively.

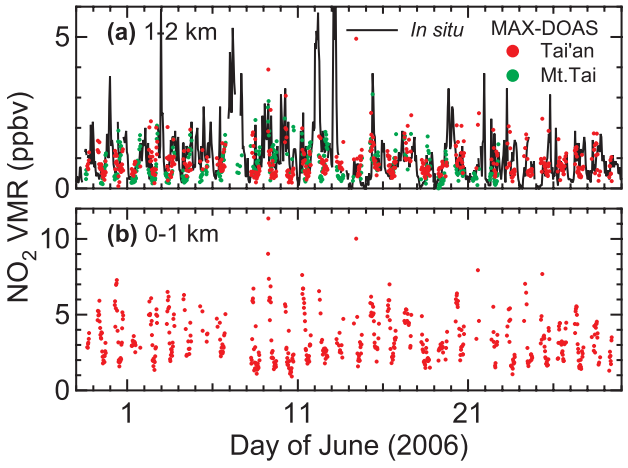

Fig. 5. **(a)** Time series of the mean NO_2 volume mixing ratios (VMRs) for the 1-2-km layer above the surface (∼1.6±0.5 km a.s.l.) derived from MAX-DOAS measurements at Tai'an (red) and Mt. Tai (green). In situ NO_2 data obtained at the top of Mt. Tai (∼1.5 km a.s.l.) are also shown in black. **(b)** Time series of the mean NO_2 VMRs derived from MAX-DOAS measurements at Tai'an is shown for the 0–1-km layer above the surface.

to aerosols (and potentially clouds) do not show distinct differences in spatial inhomogeneity between cases of MODIS AODs less and greater than 1.2, suggesting that most of the comparisons have been made under cloud-free conditions. Therefore, it is most likely that the significant deviations seen at MODIS AOD>1.2 were caused by the presence of high-altitude optically thick aerosols (above ∼2 km), to which the sensitivity of MAX-DOAS measurements was too low. However, the 30% change in MAX-DOAS AOD influences the retrieved NO_2 VCD and VMR by only about 10% (Table 1), indicating that an underestimate in MAX-DOAS AOD is a minor problem for the NO_2 retrievals. This is confirmed below by making additional comparisons with in situ NO_2 measurements performed at the summit of Mt. Tai.

Figure 5a shows two sets of MAX-DOAS NO_2 VMR data from Tai'an and Mt. Tai, which are compared with in situ NO_2 VMR data. The data plotted are the mean NO_2 VMRs at 1–2 km above the surface (1626±500 m a.s.l.; Tai'an is at 126 m a.s.l.) for MAX-DOAS measurements and the NO_2 VMRs at the mountain top (1534 m a.s.l) for the in situ measurements. Thus, air masses measured by these MAX-DOAS and in situ instruments differed, especially in terms of the representative altitude and air mass volume. These differences made it difficult to assess the MAX-DOAS data using a correlation analysis. We find, however, that on average these different datasets show very similar values (Fig. 5a). The mean differences of NO_2 VMRs measured by MAX-DOAS instruments at Tai'an and Mt. Tai from in situ NO_2 data were as small as -0.01 ± 0.60 ppbv and -0.29 ± 0.65 ppbv, respectively, where in situ NO_2 data showed that the mean NO_2 VMR was about 1 ppbv. These agreements provide confidence in our MAX-DOAS retrieval methods and hence the accuracy of MAX-DOAS NO_2 VMRs at 0–1 km, shown in Fig. 5b, because the sensitivity of MAX-DOAS measurements at Tai'an to the layer of 0–1 km should be much higher than that to the 1–2-km layer (Table 1), as discussed earlier. This further ensures the accuracy of the MAX-DOAS tropospheric NO_2 column data, because in general most NO_2 should be at altitudes below 2 km and our MAX-DOAS retrieval algorithm takes into account the profile above 2 km as well.

3.2 Diurnal variation of tropospheric NO_2

For the period from 29 May to 29 June 2006, the time series plot of the tropospheric NO_2 VCDs derived from MAX-DOAS measurements at Tai'an is shown in Fig. 6. The median tropospheric VCD for the period was 9.4×10^{15} molecules cm^{-2}, where the central 67% of the data were widely distributed between 6.1×10^{15} and 15.7×10^{15} molecules cm^{-2}. The large temporal variation of NO_2 observed here was caused predominantly by its diurnal variation, not day-to-day variation, as seen in Fig. 6. To quantify the diurnal variation, the hourly median tropospheric NO_2 VCDs measured by MAX-DOAS are plotted against the local time of the measurements (Chinese standard time, CST) in Fig. 7a. To characterize the OMI data from the viewpoint of the diurnal variation pattern, the mean value of OMI NO_2 tropospheric VCDs obtained at locations within

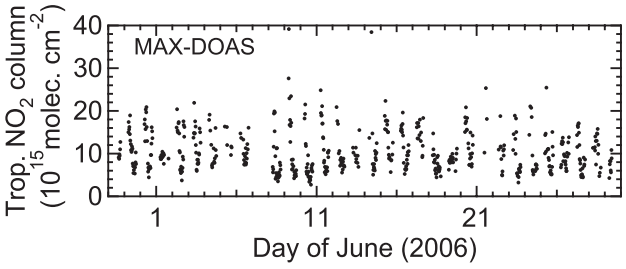

Fig. 6. Time series of all the MAX-DOAS data of tropospheric NO_2 columns at Tai'an.

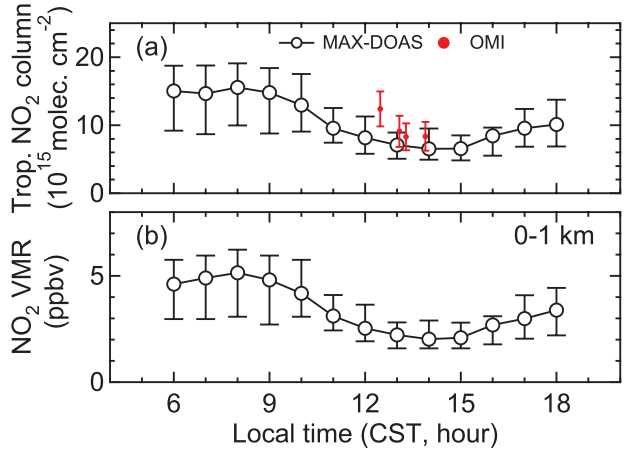

Fig. 7. **(a)** Median diurnal variation of the tropospheric NO_2 columns measured by MAX-DOAS at Tai'an over the period from 29 May to 29 June 2006. Error bars represent 67% ranges. Mean values of OMI tropospheric columns obtained within 0.1° latitude and longitude of Tai'an are also plotted in red, for 8, 16, 18, and 26 June 2006. For each day, the mean error over Tai'an is shown with error bars. The local time is the Chinese standard time. **(b)** Same as (a), but for the median MAX-DOAS NO_2 VMR values for the 0–1-km layer above the surface.

0.1° latitude and longitude of Tai'an is also plotted for each of 8, 16, 18, and 26 June 2006.

As seen in Fig. 7, MAX-DOAS measurements provided the complete diurnal variations of the NO_2 tropospheric VCD and VMR at 0–1 km in daytime. The tropospheric NO_2 VCD (VMR at 0–1 km) was highest at $\sim 15 \times 10^{15}$ molecules cm^{-2} ($\sim$5 ppbv) in the early morning (6:00–9:00 CST) and dropped to $\sim 7 \times 10^{15}$ molecules cm^{-2} ($\sim$2 ppbv) at 13:00–15:00 ST. This indicates that the OMI measurements were made when the tropospheric NO_2 VCD was lowest in its typical diurnal cycle.

Interestingly, the diurnal variation pattern in the tropospheric NO_2 VCD measured by MAX-DOAS indicates that the ratio of the tropospheric VCDs at 10:00 and 13:30 LTs was greater than unity, consistent with that derived from two different types of satellite measurements (by SCIAMACHY

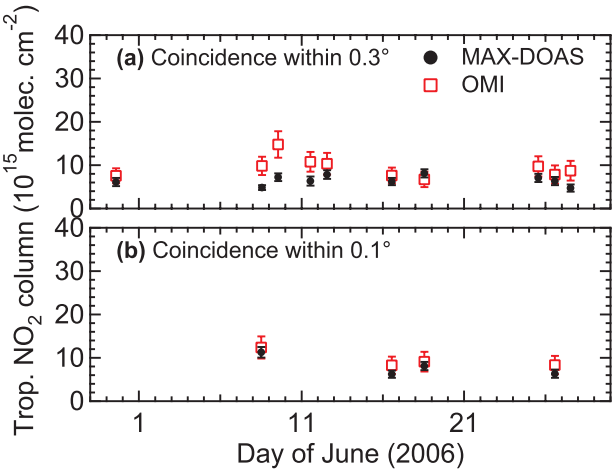

Fig. 8. Coincident pairs of Tai'an MAX-DOAS (black) and OMI (red) selected with coincident location criteria of **(a)** 0.3° and **(b)** 0.1°. The mean OMI value over Tai'an is plotted for each day. Error bars represent the mean error range over Tai'an.

around 10:00 LT and OMI around 13:30 LT) and that simulated by the GEOS-Chem model for northeastern China in August 2006 (Boersma et al., 2008). The ratio derived from MAX-DOAS measurements for June 2006 was $\sim$1.9, which was greater than those from SCIAMACHY/OMI measurements ($\sim$1.4) and the GEOS-Chem model ($\sim$1.3) for August 2006, probably due to the different photochemical loss rate and/or diurnal variation pattern of the NO_x emission between the two periods. The difference might occur also due to the difference between the diurnal variation over Tai'an, a city in NCP (for MAX-DOAS), and the mean diurnal variation over the entire northeastern China (for SCIAMACHY/OMI and GEOS-Chem).

3.3 Validation of OMI data

In Fig. 8a, the day-by-day variation of the mean OMI tropospheric NO_2 VCDs obtained at locations within 0.3° latitude and longitude of Tai'an is plotted together with MAX-DOAS tropospheric NO_2 column data. MAX-DOAS values were obtained by interpolating two values measured within 30 min before and after OMI measurements were made. Using this coincidence criterion results in 10 coincident MAX-DOAS/OMI pairs (Fig. 8a). The number of coincident pairs was reduced to 4 when a coincident location criterion of 0.1° was used instead (Fig. 8b). For either case the OMI data show a temporal variation much smaller than that seen in all the MAX-DOAS data (Fig. 6), as the OMI measurements were made only at specific LTs.

For cases with a coincidence criterion of 0.3°, we find that the correlations between tropospheric NO_2 VCDs derived from MAX-DOAS and OMI are rather poor (Fig. 9). This should be partly because the tropospheric

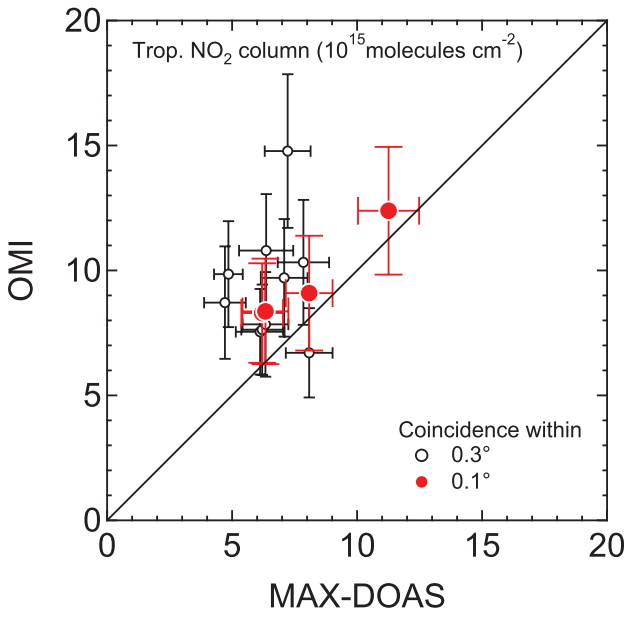

Fig. 9. Correlations between tropospheric NO_2 columns derived from MAX-DOAS and OMI. The pairs selected by the different coincident criteria of 0.3° and 0.1° are shown in black and red, respectively. Error bars represent the respective error ranges.

NO_2 VCD at OMI measurement LTs was invariant over the limited time period analyzed here. The mean difference ($\pm 1\sigma$ standard deviation) between OMI and MAX-DOAS (OMI minus MAX-DOAS) was estimated to be $(+2.9\pm2.5)\times10^{15}$ molecules cm^{-2} (+45±38%). In contrast, the use of a stricter coincident location criterion of 0.1° considerably improves the agreement, with a resulting mean difference as small as $(+1.6\pm0.6)\times10^{15}$ molecules cm^{-2} (+20±8%). This suggests that such a strict coincidence criterion is a prerequisite for accurate validation comparisons, especially over areas containing a city or a mountain, which can increase the NO_2 spatial inhomogeneity.

On the basis of the results for a coincident criterion of 0.1°, it is likely that on average OMI tropospheric NO_2 data are biased high by 1.6×10^{15} molecules cm^{-2} (20%), at least for the locations and the time period of the comparisons made here. However, the differences are less than the reported error of the OMI data (Fig. 9). Although the number of coincident MAX-DOAS/OMI pairs is small, these results are supported by the fact that the comparisons have been made only for 8, 16, 18, and 26 June, when the MAX-DOAS AODs show good agreement with MODIS data (Fig. 3).

Celarier et al. (2008) have summarized results of the validation of OMI tropospheric NO_2 data for the US, Europe, and Pacific Ocean using coincident measurements, including MAX-DOAS measurements during the DANDELIONS (Dutch Aerosol and Nitrogen Dioxide Experiments for Validation of OMI and SCIAMACHY) (Brinksma et al., 2008) campaign, aircraft measurements during the INTEX (Intercontinental Chemical Transport Experiment)-A, PAVE (Polar Aura Validation Experiment), and INTEX-B campaigns (Bucsela et al., 2008), and the Multi-Function DOAS (MF-DOAS) measurements during the INTEX-B campaign. They investigated the correlations of OMI data with coincident measurement data and concluded that OMI tropospheric NO_2 column data likely have a negative bias of 15–30%, based on the slope of the linear regression line. It should be noted, however, that some comparisons, especially with MAX-DOAS measurements, revealed that the regression lines have an intercept of $(3\pm1)\times10^{15}$ molecules cm^{-2}, suggesting a positive bias of OMI values. Thus, the bias of OMI data is likely nonconstant over a wide range of tropospheric NO_2 column values. In addition, the bias can vary over different regions, for example, through the AMF computation assuming a spatial distribution of the surface albedo. Furthermore, the bias may have a seasonality (Lamsal et al., 2008). Despite these complicated dependencies, however, it is reasonable to conclude here that the OMI tropospheric NO_2 column data have a bias of +20/−30%, which accounts for both our results and the above-mentioned other validation results. To confirm this and diagnose a potential cause of the bias, a more detailed investigation and more robust comparisons covering a wide range of tropospheric NO_2 columns and different locations would be necessary.

4 Conclusions

To validate the OMI tropospheric NO_2 column data (the standard product, version 3) obtained over the North China Plain (NCP) for the first time, we performed satellite-independent measurements of the tropospheric NO_2 column using ground-based MAX-DOAS instruments at two sites (Tai'an and Mt. Tai) in NCP from 29 May to 29 June 2006. For each retrieval of the tropospheric NO_2 column from MAX-DOAS measurements, we used the box-air-mass-factor vertical profiles determined by analyzing the absorption of O_4 with our DOAS method and aerosol retrieval algorithm (Irie et al., 2008). While the AOD values derived from MAX-DOAS O_4 measurements agreed with MODIS AOD values to within 30% for most cases, MAX-DOAS AOD values tended to be underestimated at MODIS AOD>1.2, due to less sensitivity of the MAX-DOAS measurements to high-altitude aerosols (above ∼2 km). However, comparisons between the mean NO_2 VMRs measured by the Tai'an MAX-DOAS for the 1-km layer centered at ∼1.6 km with those measured by an in situ instrument at the summit of Mt. Tai (∼1.5 km) showed that the differences were as small as −0.01±0.60 ppbv, supporting the accuracy of MAX-DOAS tropospheric NO_2 data. MAX-DOAS provided the complete diurnal variation of the NO_2 tropospheric VCD (and VMR in the layer for 0 to 1 km) in daytime, with a maximum of $\sim15\times10^{15}$ molecules cm^{-2} (∼5 ppbv) at 6:00–9:00 CST

and a minimum of $\sim 7\times10^{15}$ molecules cm^{-2} ($\sim$2 ppbv) at 13:00–15:00 CST, characterizing the OMI measurements made at specific LTs around 13:30. Agreement between tropospheric NO_2 columns measured by OMI and MAX-DOAS was improved using a stricter coincident location criterion of 0.1°. The mean difference ($\pm1\sigma$ standard deviation) between OMI and MAX-DOAS (OMI minus MAX-DOAS) was then estimated to be $(+1.6\pm0.6)\times10^{15}$ molecules cm^{-2} ($+20\pm8$%). Considering other validation results for the US, Europe, and Pacific Ocean (Brinksma et al., 2008; Bucsela et al., 2008; Celarier et al., 2008), the bias was estimated to be +20/−30%, which may depend on the region. These estimates provide the quantitative basis necessary for analyzing OMI data, especially over NCP.

Acknowledgements. The standard product (SP) of OMI NO_2 data was obtained from the NASA Goddard Earth Sciences Data and Information Services Center (GES-DISC). MODIS data were obtained from the NASA LAADS web site. This work was supported by the Global Environment Research Fund (B-051) of the Ministry of the Environment, Japan. This work was supported by the Ministry of Education, Culture, Sports, Science and Technology (MEXT). This work was supported by Japan EOS (Earth Observation System) Promotion Program of the Ministry of Education, Culture, Sports, Science and Technology (MEXT).

Edited by: M. Van Roozendael

References

Boersma, K. F., Eskes, H. J., and Brinksma, E. J.: Error analysis for tropospheric NO_2 retrieval from space, J. Geophys. Res., 109, D04311, doi:10.1029/2003JD003962, 2004.

Boersma, K. F., Jacob, D. J., Eskes, H. J., Pinder, R. W., Wang, J., and van der A, R. J.: Intercomparison of SCIAMACHY and OMI tropospheric NO_2 columns: Observing the diurnal evolution of chemistry and emissions from space, J. Geophys. Res., 113, D16S26, doi:10.1029/2007JD008816, 2008.

Brinksma, E. J., Pinardi, G., Braak, R., Volten, H., Richter, A., Schönhardt, A., van Roozendael, M., Fayt, C., Hermans, C., Dirksen, R. J., Vlemmix, T., Berkhout, A. J. C., Swart, D. P. J., Oetjen, H., Wittrock, F., Wagner, T., Ibrahim, O. W., de Leeuw, G., Moerman, M., Curier, R. L., Celarier, E. A., Knap, W. H., Veefkind, J. P., Eskes, H. J., Allaart, M., Rothe, R., Piters, A. J. M., and Levelt, P. F.: The 2005 and 2006 DANDELIONS NO_2 and aerosol validation campaigns, J. Geophys. Res., 113, D16S46, doi:10.1029/2007JD008808, 2008.

Bucsela, E. J., Celarier, E. A., Wenig, M. O., Gleason, J. F., Veefkind, J. P., Boersma, K. F., and Brinksma, E.: Algorithm for NO_2 vertical column retrieval from the Ozone Monitoring Instrument, IEEE Trans. Geosci. Remote Sens., 44, 5, 1–14, 2006.

Bucsela, E. J., Perring, A. E., Cohen, R. C., Boersma, K. F., Celarier, E. A., Gleason, J. F., Wenig, M. O., Bertram, T. H., Wooldridge, P. J., Dirksen, R., and Veefkind, J. P., Comparison of tropospheric NO_2 from in situ aircraft measurements with near-real-time and standard product data from OMI, J. Geophys. Res., 113, D16S31, doi:10.1029/2007JD008838, 2008.

Celarier, E. A., Brinksma, E. J., Gleason, J. F., Veefkind, J. P., Cede, A., Herman, J. R., Ionov, D., Goutail, F., Pommereau, J. -P., Lambert, J. -C., van Roozendael, M., Pinardi, G., Wittrock, F., Schönhardt, Richter, A., Ibrahim, O. W., Wagner T., Bojkov, B., Mount, G., Spinei, E., Chen, C. M., Pongetti, T. J., Sander, S. P., Bucsela, E. J., Wenig, M. O., Swart, D. P. J., Volten, H., Kroon, M., and Levelt, P. F.: Validation of Ozone Monitoring Instrument nitrogen dioxide columns, J. Geophys. Res., 113, D15S15, doi:10.1029/2007JD008908, 2008.

Frieß, U., Monks, P.S., Remedios, J. J., Rozanov, A., Sinreich, R., Wagner, T., and Platt, U.: MAX-DOAS O_4 measurements: A new technique to derive information on atmospheric aerosols: 2. Modeling studies, J. Geophys. Res., 111, D14203, doi:10.1029/2005JD006618, 2006.

Fu, T. -M., Jacob, D. J., Palmer, P. I., Chance, K., Wang, Y. X., Barletta, B., Blake, D. R., Stanton, J. C., and Pilling, M. J.: Space-based formaldehyde measurements as constraints on volatile organic compound emissions in east and south Asia and implications for ozone, J. Geophys. Res., 112, D06312, doi:10.1029/2006JD007853, 2007.

Hönninger, G., von Friedeburg, C., and Platt, U.: Multi axis differential optical absorption spectroscopy (MAX-DOAS), Atmos. Chem. Phys., 4, 231–254, 2004, http://www.atmos-chem-phys.net/4/231/2004/.

Inomata, S., Tanimoto, H., Kameyama, S., Tsunogai, U., Irie, H., Kanaya, Y., and Wang, Z.: Technical Note: Determination of formaldehyde mixing ratios in air with PTR-MS: laboratory experiments and field measurements, Atmos. Chem. Phys., 8, 273–284, 2008, http://www.atmos-chem-phys.net/8/273/2008/.

Irie, H., Sudo, K., Akimoto, H., Richter, A., Burrows, J. P., Wagner, T., Wenig, M., Beirle, S., Kondo, Y., Sinyakov, V. P., and Goutail, F.: Evaluation of long-term tropospheric NO_2 data obtained by GOME over East Asia in 1996–2002, Geophys. Res. Lett., 32, L11810, doi:10.1029/2005GL022770, 2005.

Irie, H., Kanaya, Y., Akimoto, H., Iwabuchi, H., Shimizu, A., and Aoki, K.: First retrieval of tropospheric aerosol profiles using MAX-DOAS and comparison with lidar and sky radiometer measurements, Atmos. Chem. Phys., 8, 341–350, 2008, http://www.atmos-chem-phys.net/8/341/2008/.

Iwabuchi, H.: Efficient Monte Carlo methods for radiative transfer modeling, J. Atmos. Sci., 63, 9, 2324–2339, 2006.

Jacobson, M. Z.: Fundamentals of atmospheric modeling, Cambridge University Press, 1999.

Kurucz, R. L., Furenlid, I., Brault, J., and Testerman, L.: Solar flux atlas from 296 to 1300 nm, Natl. Sol. Obs., Sunspot, New Mexico, 240 pp., 1984.

Lamsal, L. N., Martin, R. V., van Donkelaar, A., Steinbacher, M., Celarier, E. A., Bucsela, E., Dunlea, E. J., and Pinto, J. P.: Ground-level nitrogen dioxide concentrations inferred from the satellite-borne Ozone Monitoring Instrument, J. Geophys. Res., 113, D16308, doi:10.1029/2007JD009235, 2008.

Levelt, P. F., van den Oord, G. H. J., Dobber, M. R., Mälkki, A., Visser, H., de Vries, J., Stammes, P., Lundell, J. O. V., and Saari, H.: The Ozone Monitoring Instrument, IEEE Trans. Geosci. Remote Sens., 44, 5, 1093–1101, 2006.

Marchuk, G., Mikhailov, G., Nazaraliev, M., Darbinjan, R., Kargin, B., and Elepov, B.: The Monte Carlo Methods in Atmospheric Optics, Springer-Verlag Berlin, 208 pp., 1980.

Remer, L. A., Kaufman, Y. J., Tanré, D., Mattoo, S., Chu, D. A., Martins, J. V., Li, R. -R., Ichoku, C., Levy, R. C., Kleidman, R. G., Eck, T. F., Vermote, E., and Holben, B. N.: The MODIS aerosol algorithm, products, and validation, J. Atmos. Sci., 62, 947–973, doi:10.1175/JAS3385.1, 2005.

Richter, A., Burrows, J. P., Nüß, H., Granier, C., and Niemeier, U.: Increase in tropospheric nitrogen dioxide over China observed from space, Nature, 437, 129–132, doi:10.1038/nature04092, 2005.

Rodgers, C. D.: Inverse methods for atmospheric sounding: Theory and practice, Ser. Atmos. Oceanic Planet. Phys., 2, edited by: F. W. Taylor, World Sci., Hackensack, N. J., 2000.

van der A, R. J., Peters, D. H. M. U., Eskes, H., Boersma, K. F., van Roozendael, M., de Smedt, I., and Kelder, H. M.: Detection of the trend and seasonal variation in tropospheric NO_2 over China, J. Geophys. Res., 111, D12317, doi:10.1029/2005JD006594, 2006.

van Noije, T. P. C., Eskes, H. J., Dentener, F. J., Stevenson, D. S., Ellingsen, K., Schultz, M. G., Wild, O., Amann, M., Atherton, C. S., Bergmann, D. J., Bey, I., Boersma, K. F., Butler, T., Cofala, J., Drevet, J., Fiore, A. M., Gauss, M., Hauglustaine, D. A., Horowitz, L. W., Isaksen, I. S. A., Krol, M. C., Lamarque, J.-F., Lawrence, M. G., Martin, R. V., Montanaro, V., Müller, J.-F., Pitari, G., Prather, M. J., Pyle, J. A., Richter, A., Rodriguez, J. M., Savage, N. H., Strahan, S. E., Sudo, K., Szopa, S., and van Roozendael, M.: Multi-model ensemble simulations of tropospheric NO_2 compared with GOME retrievals for the year 2000, Atmos. Chem. Phys., 6, 2943–2979, 2006, http://www.atmos-chem-phys.net/6/2943/2006/.

Wagner, T., Burrows, J. P., Deutschmann, T., Dix, B., von Friedeburg, C., Frie, U., Hendrick, F., Heue, K.-P., Irie, H., Iwabuchi, H., Kanaya, Y., Keller, J., McLinden, C. A., Oetjen, H., Palazzi, E., Petritoli, A., Platt, U., Postylyakov, O., Pukite, J., Richter, A., van Roozendael, M., Rozanov, A., Rozanov, V., Sinreich, R., Sanghavi, S., and Wittrock, F.: Comparison of box-air-mass-factors and radiances for Multiple-Axis Differential Optical Absorption Spectroscopy (MAX-DOAS) geometries calculated from different UV/visible radiative transfer models, Atmos. Chem. Phys., 7, 1809–1833, 2007, http://www.atmos-chem-phys.net/7/1809/2007/.